ACS OMEGA

http://pubs.acs.org/journal/acsodf

Article

To Explore the Binding Affinity of Human γ-Secretase Activating Protein (GSAP) Isoform 4 with APP-C99 Peptides

Deekshi Angira, Sonali Chaudhary, Arumugam Abiramasundari, and Vijay Thiruvenkatam*

Cite This: *ACS Omega* 2023, 8, 13435−13443

Read Online

ACCESS | Metrics & More | Article Recommendations | Supporting Information

ABSTRACT: γ-Secretase activating protein (GSAP) is known to play an important role in the β-amyloid pathway. It acts as a modulator and accentuates the truncation of the amyloid precursor protein C-99 fragment through the γ-secretase complex. GSAP has four isoforms, out of which canonical isoform 1, a 16 kDa C-terminal portion, has been extensively studied, whereas the function of other three isoforms remains unknown. Here, we explore the GSAP isoform 4 (GSAP_I4) expression and purification from inclusion bodies followed by the refolding of the protein. The secondary structure of GSAP_I4 is predicted using circular dichroism. The protein is further characterized by western blotting and mass spectroscopy analysis. Additionally, biochemical assays and in silico molecular docking and molecular simulation are performed to investigate the binding of GSAP_I4 and APP-C99 peptide fragments. The results reflect that although GSAP_I1 and GSAP_I4 share high sequence similarity, the isoform 4 does not show any affinity toward APP-C99 peptide fragments. This hints toward the fact that GSAP_I4 might have a different role in the living system that is yet unexplored.

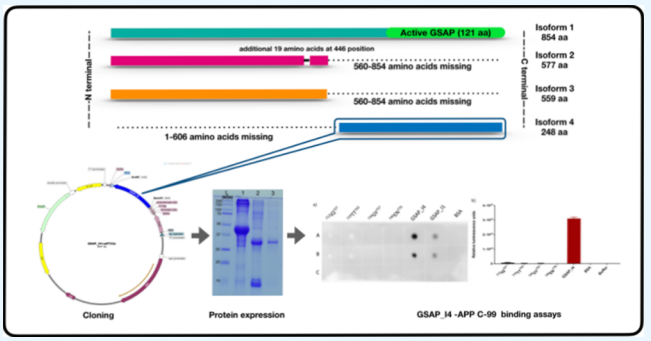

INTRODUCTION

Human genome is a complex entity that is supplemented by the alternative splicing of precursor mRNA.[1] According to the mRNA-Seq and EST-cDNA sequence data analysis, ∼95% of multiexon genes undergo alternative splicing and there are approximately 100,000 intermediate- to high-abundance alternative splicing events in major human tissues.[2] Defying the one gene-one protein notion, the expression of these alternative isoforms is usually tissue-specific; it can be directed during differentiation or can be an outcome of some external stimuli.[3,4] The protein isoforms generated as a result of alternative splicing can have different primary structure, thereby, leading to an alteration in the protein properties including protein−protein interaction, enzymatic behavior, or their folding ability.[5] One such example is 4.1R 10 kDa protein, where, among the four isoforms, the 4.1R isoform stimulates the association with fodrin/actin followed by 4.1G-SAB with 2-fold reduced efficiency. The other two isoforms 4.1N and 4.1B do not show this property.[6] Similarly, PEX5 protein has two isoforms, PEX5L and PEX5S; the former isoform PEX5L contains additional 37 amino acids and can interact with proteins containing the type-2 peroxisomal targeting signal, whereas latter is incapable to perform a similar function.[7] Minor changes in the alternative splicing can be intolerable for human life and can lead to detrimental disorders like amyotrophic lateral sclerosis, myotonic dystrophy, and cancer.[8] Protein isoforms possess the ability to express at different concentrations in a cell and perform similar or different biological roles despite sequence homology.[9] According to the study published by Yang et al. in 2016, isoform-specific regions can lead to similar or different interactions with other binding partners thereby affecting the function of two different isoforms for same protein.[10] In addition, in comparison to the canonical forms, there is barely any information available for the functional ability of most of the isoforms of a specific protein. This information can include the expression of the isoform, its role in the biological system, or its localization to count a few.[11] Therefore, it is of utmost importance to identify the isoforms and explore their behavior.

This work focuses on exploring γ-secretase activating protein isoform 4 (GSAP_I4). γ-Secretase activating protein from *Homo sapiens* has four spliced variants or isoforms starting from GSAP isoform 1 to GSAP isoform 4. Each isoform varies with a different number of amino acids: isoform 1−854 amino acids, isoform 2−577 amino acids, isoform 3−559 amino acids, and isoform 4−248 amino acids (see Figure 1). Previous studies performed on the canonical form of GSAP facilitated the investigation of the active 16 kDa GSAP_I1 as a major key

Received: February 19, 2023
Accepted: March 14, 2023
Published: March 27, 2023

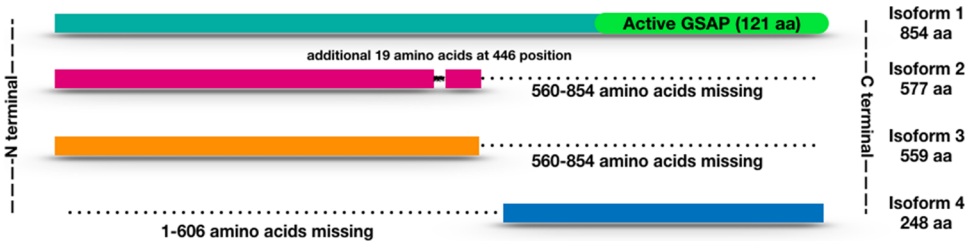

Figure 1. Image depicting the four isoforms of γ-secretase activating protein. GSAP isoform 1 (teal color) has 854 amino acids, and the active form of GSAP comprises 121 amino acids toward the C-terminal (green color). Isoform 2 (pink color) has 577 amino acids with few differences; it has 19 additional amino acids at 446 position, K is replaced by V at 559 position and 560−854 aa are missing. Isoform 3 (orange color), just like isoform 2, has K replaced by V at 559 position with 560−854 amino acids missing. Isoform 4 (blue color) has 248 amino acids, 1−606 aa are missing from the N-terminal, and it shares 100% similarity with GSAP isoform 1 with 127 extra amino acids toward the N-terminal.

player in the β-amyloid pathway and revealed that it has the ability to interact with APP-C99 fragment as well as presenilin in γ-secretase complex, followed by the γ-secretase cleavage.[12,13] γ-Secretase activating protein was discovered in the year 2010,[14] wherein the pull-down assays indicated its involvement in the β-amyloid pathway. Also, it was hypothesized that 16 kDa GSAP_I1 activates γ-secretase and is inhibited by an anticancer drug, imatinib. Hence, it is a profound target for Alzheimer's disease that has the capability to reduce the deposition of amyloid plaques.[15] Further studies conducted in the year 2014 by Chu et al. reported the role of caspase-3 and 5-lipoxygenase in the generation of 16 kDa active GSAP protein from full-length 98 kDa GSAP at ^{737}DLD^{739} caspase processing domain (cpd). Also, the degradation for GSAP was reported by the ubiquitin-proteasome pathway with a half-life of 5 h.[16−18] In addition to its role in amyloid cascade, GSAP is enriched in the mitochondria-associated membrane, thereby promoting the APP C-terminal fragment partitioning into lipid rafts that enhance Aβ production. Moreover, it is known to regulate APP phosphorylation and trafficking by its interaction with Fe65-APP complex.[19] In another study, miR-4422-5p, a novel potential diagnostic biomarker for AD, is reported to directly target the 3′UTR of GSAP and negatively regulates the protein level in vitro.[20] Although GSAP_I1 has been comprehensively characterized in the literature, there are no reports for any of the three isoforms for GSAP hitherto. As discussed earlier, GSAP_I4 has 248 amino acids, and interestingly, the C-terminal of GSAP_I4 shares 100% sequence similarity with the active 16 kDa GSAP isoform 1 consisting of 121 amino acids. This acted as the basis and motivation for us to study this isoform and explore its involvement in the living organism, initially in the prokaryotic system and later eukaryotic system as the future perspective. Therefore, the work here concentrates on probing GSAP_I4 by studying its expression in a prokaryotic protein expression system followed by the characterization and protein-peptide interaction assays to establish the function in the cell. To validate the same, GSAP isoform 4 protein was also subjected to molecular dynamics (MD) simulations.

RESULTS AND DISCUSSION

***GSAP_I4* Gene Synthesis and Sequence Validation.** The sequence for GSAP_I4 was retrieved from Universal Protein Resource (UniProt)[21] with the id A4D1B5. T-Coffee server was utilized to align the sequence of GSAP isoform 4 to the canonical GSAP isoform 1. As seen in Figure S1, the percent identity matrix calculated the identity as 100%. The *GSAP_I4* gene construct in pET-32a(+) (Figure S2) was received from GenScript and was analyzed on 0.8% agarose gel. The presence of GSAP_I4 in the expression vector was confirmed using a sequencing service from Scigenom (Supporting Data 1). The subsistence of the gene was also validated using restriction digestion. EcoRI and BamHI were used to digest the GSAP_I4 gene from the pET-32a(+) vector, and the result was analyzed on 0.8% agarose gel. A band at ∼756 base pair size was visible when viewed using a Syngene Gel Doc system (Figure 2), which confirmed the enclosure of *GSAP_I4* gene in the vector at the required site.

GSAP_I4 Expression, Purification, and Refolding. The protein expression was monitored at varying IPTG concentrations (0.1−1 mM) and temperature conditions (16−37 °C). The tagged GSAP_I4 protein expressed as inclusion bodies in

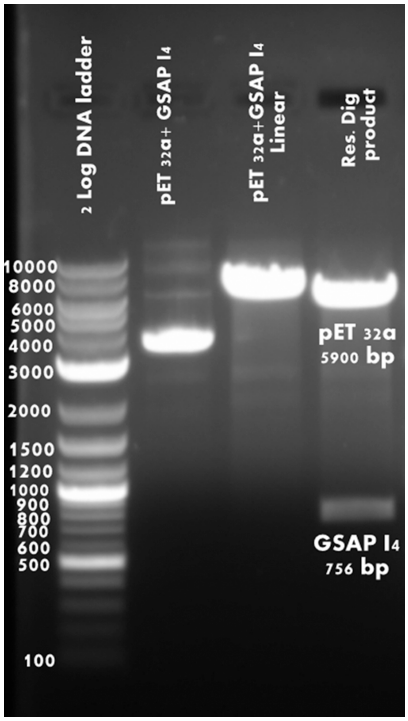

Figure 2. Agarose gel image (0.8%) showing Lane 1: 2 Log DNA ladder, Lane 2: pET-32a_GSAP_I4 plasmid at 6.6 kb, Lane 3: Linearized pET-32a_GSAP_I4 plasmid digested after restriction digestion using BamHI restriction enzyme, and Lane 4: pET-32a vector at 5.9 kb and GSAP_I4 at 0.7 kb after double digestion using BamHI and EcoRI restriction enzymes. (Uncropped image of this agarose gel is shown in Supporting Material; Figure S3).

https://doi.org/10.1021/acsomega.3c01117
ACS Omega 2023, 8, 13435−13443

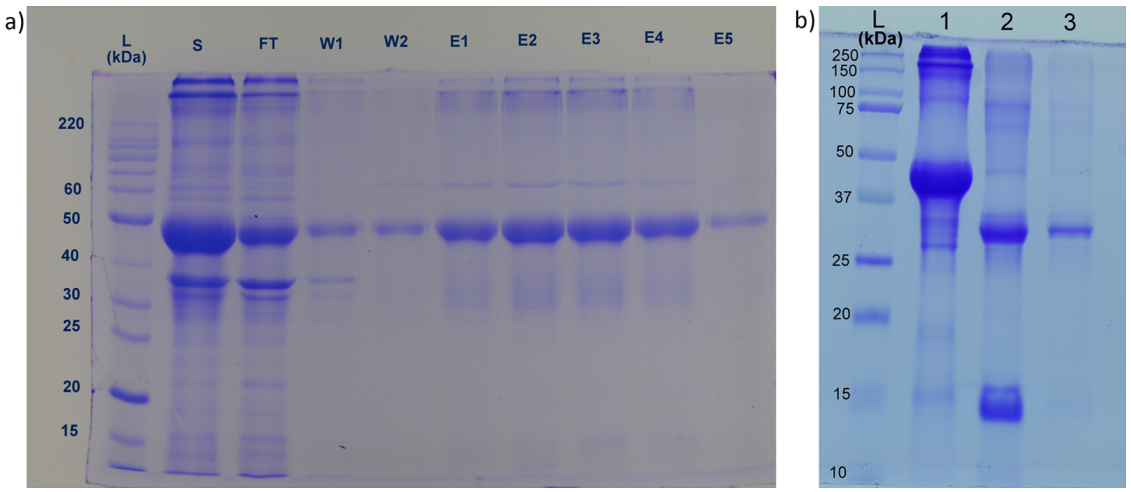

Figure 3. (a) SDS-PAGE gel image showing Trx-GSAP_I4 protein expression and purification from inclusion bodies. Lane 1: Protein marker; Lane 2: Crude sample; Lane 3: Flow through; Lane 4−5: Wash; Lane 6−10: Purified Trx-GSAP_I4 protein. (b) SDS-PAGE gel image showing Lane 1: Protein marker; Lane 2: Dialyzed Trx-GSAP_I4 (44 kDa); Lane 3: Cleaved GSAP_I4 (30 kDa) and Trx (12 kDa) after tag removal using thrombin protease; Lane 4: FPLC purified GSAP_I4 (~30 kDa) (repeated SDS-PAGE images for the above purifications are shown in Supporting Material; Figure S5).

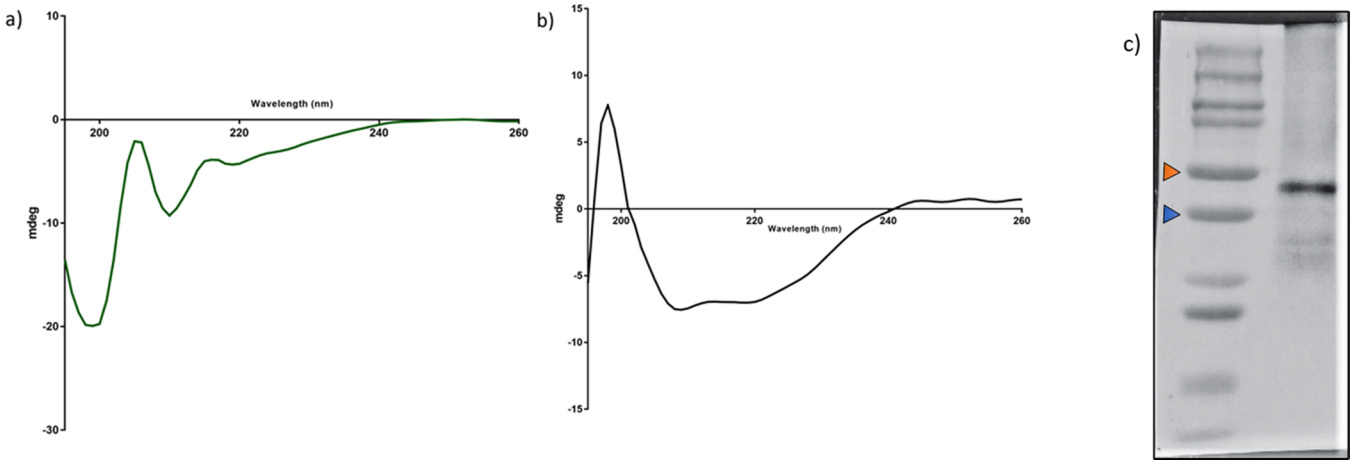

Figure 4. Image showing (a) CD spectra for denatured Trx_GSAP_I4. (b) CD spectra for refolded cleaved GSAP_I4. (c) Western blot for Trx_GSAP_I4 using anti-PION primary antibody. The orange triangle and blue triangle represent 50 and 37 kDa mark, respectively.(Uncropped image for the western blot is shown in Supporting Material; Figure S7).

all the tested conditions, with maximum expression at 25 °C at 0.5 mM IPTG (Figure S4). This result was comparable to the 16 kDa GSAP isoform 1 expression and purification that resulted in protein expression as inclusion bodies despite several attempts to solubilize it.[22] The protein purification from inclusion bodies was performed with a culture volume of 2 L. 8 M urea was used as the denaturant, and we were able to observe the Trx_GSAP_I4 band at the 43 kDa position on sodium dodecyl sulfate poly acrylamide gel electrophoresis (SDS-PAGE) after Coomassie R-250 staining. (Figure 3a).

The protein refolding was performed using a 10 kDa snake-skin dialysis membrane for 12 h at 4 °C against 1 L buffer. In order to corroborate the refolding of Trx-GSAP_I4, circular dichroism (CD) was performed for both denatured and dialyzed Trx_GSAP_I4 protein, each having a concentration of 0.2 mg/mL. The experiment was performed in triplicate, and we were able to observe the CD spectra corresponding to the proper folding of the protein. With this experiment, we confirmed that the Trx-GSAP_I4 has attained >98% proper secondary structure. The fusion protein expressed with thioredoxin at its N-terminal in the same frame with the thrombin cleavage site (LVPR/GS) in between the tag and the protein. The tag was removed using thrombin protease at 4 °C for 12 h. The proteolytic cleavage was monitored on SDS-PAGE, and the cleaved product, i.e., GSAP_I4 was successfully separated and eluted from the Trx tag using SEC-FPLC (HiLoad 16/600 Superdex 75 pg gel filtration chromatography column) with a concentration of 1.5 mg/mL. (Figure 3b).

Characterization of GSAP_I4: Secondary Structure Analysis and Western Blotting. To check for the stability of cleaved GSAP_I4 with respect to the attainment of secondary structure, 0.2 mg/mL of the sample was subjected to CD. The CD spectra indicated a properly folded secondary structure pattern with 73.91% α-helix and 1.41% β-strand, which confirmed the stability of the refolded protein. This result was in consensus with the PSI-blast-based secondary structure PREDiction (PSIPRED) analysis[23] for the GSAP_I4 sequence. As shown in Figure S6, the computation through the PSIPRED algorithm depicted 13 stretches of amino acids that had high probability to form α-helix (~68%), whereas there was just one

https://doi.org/10.1021/acsomega.3c01117
ACS Omega 2023, 8, 13435−13443

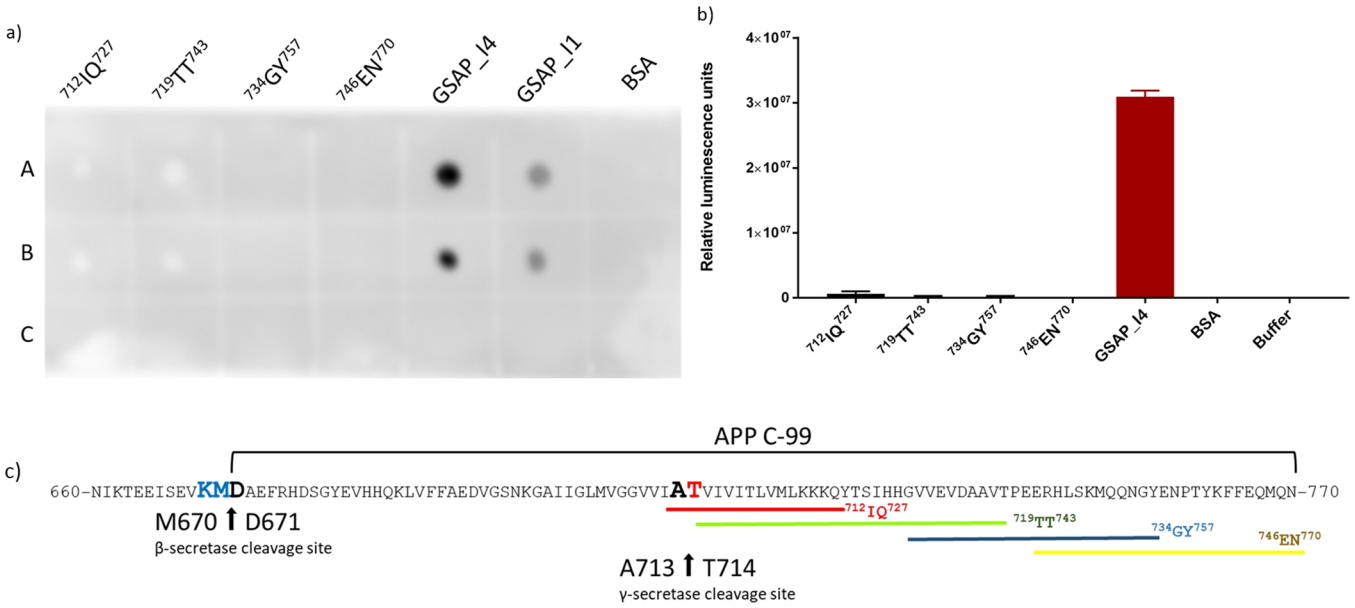

Figure 5. (a) Dot-blot far-western experiment illustrating the binding analysis with the four peptides, no binding was observed with any of the peptides. Here, Lane A: 500 μM peptide concentration, Lane B: 250 μM peptide concentration, and Lane C: 0 μM peptide concentration, as used in the experiment (b) ELISA results depicting a similar result with no binding APP-C99 fragment-based designed peptides. (c) APP-C99 fragment showing β-secretase and γ-secretase cleavage site together with the four peptides designed and depicted as ^{712}IQ^{727} in red, ^{719}TT^{743} in green, ^{734}GY^{757} in blue, and ^{746}EN^{770} in yellow color lines (repeated dot blot is shown in Supporting Material; Figure S8).

stretch of 4 amino acids that predicted β-strand secondary structural element (~1.6%). (Figure 4a,b) The protein was also characterized using western blotting by anti-PION primary antibody and antirabbit secondary antibody. The presence of the protein was detected in the form of chemiluminescence signal upon the addition of enhanced chemiluminescence (ECL) solution from Bio-Rad (Figure 4c).

Mass Spectrometry Analysis. The proteins detected by liquid chromatography electrospray ionization tandem mass spectrometry (LC ESI MS/MS) are listed with their predicted molecular mass as seen in Supporting Data 2. GSAP with Uniprot id. A4D1B5 was seen as the major hit confirming the protein identity. The number of identified peptides for the protein and the corresponding protein sequence coverage is also specified in the same table.

Immunoassays to Identify the Function for GSAP_I4. The previous work performed with GSAP isoform 1 highlights the role of the protein as a key player in the β-amyloid pathway.[14] The GSAP isoform 1 has been proven to interact with amyloid precursor protein C-99 (APP-C99) and presenilin.[12,13] Since the studies pertaining to GSAP_I4 are being reported for the first time, we wanted to investigate that owing to the sequence similarity between canonical GSAP and GSAP_I4, whether it also perceives a similar function to isoform 1.

Dot-blot far-Western analysis and indirect enzyme-linked immunosorbent analysis (ELISA) (Figure 5) were performed in order to probe the affinity of GSAP_I4 with APP-C99 peptide fragments that were designed based on the peptide scanning approach as discussed by Angira et al. in 2019.[13] Unlike, GSAP_I1 (Figure 6), we were not able to observe any binding in dot-blot-far Western or ELISA. GSAP_I1 and GSAP_I4 were used as a positive control that showed a positive signal, whereas BSA was used as a negative control that displayed no signal after incubation with a primary antibody specific for GSAP. With this observation, we can infer

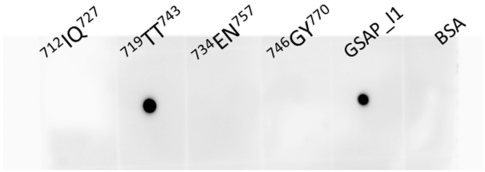

Figure 6. Dot-blot far-western experiment illustrating the binding analysis of MBP tagged GSAP_I1 with the four peptides. ^{734}TT^{743} peptide gave a positive signal for binding with the protein. Here, 250 μM of peptide concentration was used for the experiment.

that GSAP_I1 and GSAP_I4 might have different functions in the biological system despite their sequence similarity. More studies need to be performed in the future to deduce the role of GSAP_I4 using cell biology. Therefore, potential studies can focus on GSAP_I4 knockout and GSAP_I4 expression in mammalian hosts with labeled tags that can aid in studying the protein trafficking in the cell.

GSAP Isoform 4 MD Simulation Studies. As reported by Angira et al. in 2019,[13] the APP-C99 fragment (^{719}TT^{743}) binds with the N-terminal amino acid residues (amino acids 733−854) of the full-length GSAP isoform 1 protein. However, from the protein-peptide docking results for GSAP_I4 and APP-C99 (Figure S9) we observed that the ^{719}TT^{743}APP-C99 peptide bound to the active 16 kDa region for a very short span of time frame. Upon performing the MD simulation at 500 ns, the RMSD of the protein backbone (green) and the peptide (red) over the course of 500 ns appears stable (Figure S10). Rather, it was observed that the APP fragment shows comparatively better binding to the C-terminal of the GSAP isoform 4, located away from the active 16 kDa fragment. This is visible in Figure S9, where the peptide (cyan) binds in the C-terminal groove, formed due to the folding of the GSAP I4 protein. Stereochemical validation shows 85.1% residues, i.e., 194 amino acids are in allowed regions of Ramachandran plot. However, it was observed that

https://doi.org/10.1021/acsomega.3c01117
ACS Omega 2023, 8, 13435−13443

the peptide loses its helicity in the middle of the run with a presence of slight helicity by the end of the simulation (Figure S11). This can be due to nonspecific interaction between the modeled GSAP_I4 and the peptide.

CONCLUSIONS

The protein isoforms are the result of alternative splicing which is highly important for the functional diversity or complexity in eukaryotic proteome.[24] In few proteins like Piccolo, even the addition or deletion of nine amino acid residues in different spliced variants has drastically affected the property of the protein.[25] Studies have shown that the splicing rather occurs within intrinsically disordered regions of the protein that maintains the structural integrity of the protein but creates miscellany in the role of that biological macromolecule.[26] GSAP, also known as PION, comprises four isoforms. GSAP isoform 1 is the canonical form of protein that regulates the gamma secretase activity. Efforts have been made to evaluate and validate the role of GSAP in the amyloid beta pathway. Through the photophore walking approach, it has been highlighted that γ-secretase has two conformations that are regulated by GSAP. In the presence of GSAP, presenilin 1 adopts a native conformation permitting the normal processing of APP and Notch. When GSAP is knocked out, it results in a different PS1 conformation, associated with a reduction of γ-secretase activity for APP, leading to reduction in Aβ secretion.[12] A mechanistic model of γ-secretase modulation by GSAP-16 kDa through liquid−liquid phase separation indicates that in the dilute phase of GSAP-16 kDa, the recruitment of APP-C99 into γ-secretase favors the production of Aβ42. GSAP-16 kDa condensates, and droplets isolate APP-C99, thereby, making it inaccessible to γ-secretase. Hence, the protease activity is lowered eventually.[27] The proteins involved in the amyloid beta pathway such as APP, beta secretase, and gamma secretase complex, especially presenilin, are prone to mutations. Utilizing this evidence, the fit−stay−trim mechanism has been proposed where two major conformation states of APP-C99, a loose and a compact state have been identified. Compact state entails that a tight fit of APP-C99 increases the time it dwells in proximity of the enzyme, thereby leading to an extended trimming and short Aβ peptides.[28−30] In future, based on this mechanism, the binding of GSAP with presenilin or APP-C99 can be studied. With a similar idea, we aim to investigate an unknown isoform of γ-secretase activating protein. The work started with basic molecular biology, protein expression, and purification. The results evidently show that the just like GSAP isoform 1, GSAP_I4 also tends to express as inclusion bodies even after being expressed as a fusion protein with a highly stable thioredoxin tag. However, we were able to purify and refold the protein followed by the thioredoxin tag removal using thrombin protease. The refolded and cleaved GSAP_I4 protein was later assessed for its affinity and its role in the β-amyloid pathway to figure out whether it possesses a similar role to isoform 1. Through the immunoassays and in silico analysis, we inferred that GSAP_I4, unlike GSAP_I1, does not show any binding affinity for the APP-C99 fragment in the beta-amyloid pathway as reported by Angira et al. in 2019.[13] The exact role of GSAP_I4 in the biological system remains unclear. However, there are several prospective methods that can be used as a tool for protein function determination like metabolite cocktail screening,[31] protein microarray,[32] and mass spectrometry-based methods,[33] working toward the functional mechanism of GSAP isoforms can be a novel area of research and can lead to unexplored functional aspects of this protein in addition to its role in Alzheimer's disease. The characterization of unknown proteins is the foundation of translational research that ensures the accomplishment of efforts in the field of proteomics and biological science.

Materials. Luria−Bertani broth and Luria−Bertani Agar Miller were acquired from Himedia. MAX Efficiency DH5αF'IQ Competent Cells, Snake-Skin Dialysis Tubing, 10 K MWCO, 22 mm (Cat. 68,100), S.O.C. medium, and glycerol were purchased from ThermoFisher Scientific. One ShotBL21-(DE3) Competent Cells from Invitrogen and QIAprep Spin Miniprep Kit were purchased from Qiagen. Nuvia IMAC Resin, Nickel, Immunoblot PVDF western blotting Membrane, Econo-Column Chromatography Columns, and Clarity ECL western blotting Substrate from Bio-Rad, Isopropyl-β-D-1-thiogalactopyranoside (IPTG), sodium chloride (NaCl), Triton-X l00, imidazole, N, N′-methylenebisacrylamide, tetramethylethylenediamine (TEMED), ammonium per sulfate (APS), sodium dodecyl sulfate (SDS), β-mercaptoethanol (BME), bromophenol blue, Coomassie Brilliant Blue R-250, nonfat milk, nuclease-free water, urea (Cat. U5378), Ampicillin sodium salt, calcium chloride dihydrate, Trizma base, and acrylamide were purchased from Sigma-Aldrich (Darmstadt, Germany). EcoRI, BamHI-HF, and CutSmart Buffer Complete were acquired from New England Biolabs. EDTA-Free protease inhibitor tablets (Cat. 04693132001) were obtained from Roche (Basel, Switzerland). HiLoad 16/600 Superdex 75 pg gel filtration chromatography column was purchased from GE Healthcare (Chicago, Illinois, USA). An Amicon Ultra concentrator with a 10 kDa cutoff filter was obtained from Merck Millipore (Darmstadt, Germany). Anti-PION primary antibody (Cat. ab106630) was purchased from Abcam, and antirabbit IgG HRP-linked Secondary Antibody (Cat. 7074) was obtained from Cell Signaling Technology (MA, USA).

METHODS

Design and Construction of GSAP_I4 Gene in the pET-32a(+) Vector. *Pairwise Alignment.* The canonical γ-secretase activating protein comprises 854 amino acids, and the 121 amino acids from the C-terminal correspond to the active GSAP (GSAP_I1). This active GSAP sequence was aligned to the amino acid sequence of GSAP_I4 using T-coffee sequence alignment package and the percent identity matrix was generated.[34] Owing to the 100% similarity to GSAP_I1, the affordable size of GSAP_I4, and its unexplored function, the full-length gene sequence was considered for further studies.

Construction of GSAP_I4 in pET-32a(+). *GSAP* isoform 4 (*GSAP_I4*) gene inserted into the pET-32a(+) vector was obtained from GenScript. The design of a complete ORF of *GSAP_I4* from *Homo sapiens* genomic DNA into pET-32a(+) were performed as per the following instructions (Figure S2). The vector pET-32a(+) has N-terminal hexahistidine and N-terminal thioredoxin tag and has an advantage of having T7 promoter that drives the expression of the protein using lac operon, produces a high level of transcription in *E.coli*, and is not recognized by *E.coli* RNA polymerase.[35] The expression plasmid was constructed with *GSAP_I4* gene in EcoRI and BamHI restriction sites at N and C-terminal respectively. The advantage of having thioredoxin (TrxA, or Trx,) a 12 kDa intracellular thermostable protein is that it has an intrinsic oxidoreductase activity. The thioredoxin tag is expected to

https://doi.org/10.1021/acsomega.3c01117
ACS Omega 2023, 8, 13435−13443

form a protein that can be highly soluble as it produces protein in cytoplasm thereby preventing inclusion body formation.[36,37]

The synthesized gene in pET-32a(+) was received and was transformed in *E. coli* DH5α cells using the standard transformation protocol by the heat shock method.[38] The cells were made competent using the $CaCl_2$ method.[39] Transformed bacterial cells were grown on Luria−Bertani (LB) media supplemented with 50 μg/mL of ampicillin, and the plasmid was isolated using Qiagen miniprep kit. The presence of *GSAP_I4* gene in the plasmid was confirmed by DNA sequencing using Scigenom sequencing service and by restriction digestion. The prepared construct of pET-32a_GSAP_I4 was chemically transformed with calcium chloride into *Escherichia coli* BL21DE3 competent cells as well as Rosetta-gami 2(DE3)pLysS, which were plated onto LB agar using ampicillin marker (100 μg/mL) and then incubated overnight at 37 °C.

Protein Expression, Purification, and Refolding. A single colony was inoculated in 10 mL of autoclaved LB media supplemented with ampicillin and was grown overnight at 37 °C at 250 rpm. This was followed by a secondary inoculation of the 100 mL of sterile LB medium containing 100 μg/mL ampicillin, and preliminary studies were carried out to find out the optimum temperature and induction condition for protein expression. The bacterial culture was allowed to grow at 37 °C at 250 rpm until OD_{600} reached 0.5−0.6. Recombinant protein expression was then induced using isopropyl-β-D-1-thiogalactopyranoside (IPTG) (0.1−1 mM) at various temperature conditions ranging from 16° to 37 °C. The optimized condition comprised of 0.5 mM IPTG at 25 °C wherein although the expression was in inclusion bodies, yet the level of expression was significantly high as compared to other conditions. The 2 L bacterial culture was allowed to grow for 8−10 h. The cells were later harvested by centrifugation at 10,000 rpm at 4 °C for 15 min.

A three-step procedure was adopted to isolate the protein from inclusion bodies that included lysing the bacterial pellet, washing of the pellet followed by denaturation using a high concentration of denaturant, i.e., urea. The pellet was resuspended in lysis buffer (pH 8.0 Tris-Cl: 30 mM, NaCl: 300 mM, Imidazole: 10 mM, Glycerol: 10%, Triton-X 100: 0.1%). For each gram of pellet, 10 mL of lysis buffer was added, and the resuspended solution was ultrasonicated for 12 min using a Vibra-Cell sonicator (amplitude: 40% with 15 s ON and 15 s OFF cycle). The lysate was spun for 55 min at 12,000 rpm maintained at 4 °C. The supernatant was collected and analyzed for protein expression using SDS-PAGE. The pellet was again resuspended in 25 mL of lysis buffer, and the solution was centrifuged for 30 min at 13,000 rpm at 4 °C twice. The pellet obtained was washed with 15 mL of wash buffer (pH 8.0 Tris-Cl: 30 mM, NaCl: 300 mM), and the solution was centrifuged at 13,000 rpm for 20 min at 4 °C. This step was again repeated twice. The pellet was finally resuspended in 30 mL of denaturation buffer (8 M Urea, pH 8.0 Tris-Cl: 30 mM, NaCl: 300 mM, β-mercaptoethanol: 10, and 15 mM imidazole) and was incubated on a tube rotator at 20 rpm for 12 h at room temperature. The solution was centrifuged at 13,000 rpm for 45 min at 25 °C. The supernatant was collected and checked for the presence of protein on SDS-PAGE. The protein obtained was purified using the IMAC Ni-NTA column loaded with 2 mL of resin. The column was washed with Milli-Q water and pre-equilibrated with 5-column volume (CV) of column buffer (8 M Urea, pH 8.0 Tris-Cl: 30 mM, NaCl: 300, and 15 mM imidazole). The denatured protein solution was loaded onto the column followed by 200 mL of column buffer. It was then eluted using elution buffer (Urea: 8M, pH 8.0 Tris-Cl: 30 mM, NaCl: 300 mM, and imidazole: 300 mM) and analyzed by SDS-PAGE. The eluted fractions were concentrated using an Amicon Ultra-15 Centrifugal Filter Unit with an Ultracel-10 membrane to a volume of 1 mL and were dialyzed in 30 mM Tris-Cl pH 8.0, 150 mM NaCl, 50 mM imidazole pH 8.0, 5 mM β-mercaptoethanol, and 2 M urea at 4 °C for 12 h using snake-skin dialysis tubing with 10 kDa MWCO. The sample was run on SDS-PAGE for further analysis.

The thioredoxin-GSAP_I4 fusion construct was subjected to cleavage to remove the thioredoxin tag. One unit of thrombin protease was used in 2.5 mM $CaCl_2$, 50 mM Tris-Cl (pH 8.0), and 150 mM NaCl cleavage buffer. The protein with the thrombin protease was incubated at 4 °C for 12 h, and the cleaved product was separated using size exclusion chromatography.

Western blot analysis was also performed to confirm the presence of Trx-tagged GSAP_I4. The sample was run on 12% SDS-PAGE and was electro-blotted onto the prewetted PVDF membrane at 25 V for 190 min. The membrane was incubated in 5% fat-free milk in TBST for 2 h with continuous shaking to prevent nonspecific binding. The membrane was washed with TBST 4−5 times and was incubated with anti-PION rabbit polyclonal antibody with the dilution of 1:1000. The incubation was performed at 4 °C overnight with mild shaking. The membrane was then washed with TBST 4−5 times and was incubated with HRP-conjugated antirabbit secondary antibody for 2 h at room temperature on a shaker. ECL solution from Bio-Rad was used to develop the blot that was viewed using a gel documentation (gel doc) system (Bio-Rad) after 2−3 min of incubation.

Mass Spectrometry. The gel sample corresponding to GSAP_I4 was excised from the freshly run SDS-PAGE and was sent to IIT Bombay proteomics facility for LC ESI MS/MS analysis via in-gel digestion and peptide fingerprinting.

Secondary Structure Determination: CD. The refolded and cleaved GSAP_I4 protein sample (98% purity by SDS-PAGE) was filtered through 0.2-μm filters (Merck Millipore, Darmstadt, Germany). Far-UV CD spectra of the protein sample was recorded in 0.5 mm quartz cuvette at 25 °C using J-815 CD spectropolarimeter (Jasco, Inc., MD, USA) equipped with a peltier-type temperature control system at a wavelength scan of 190 to 260 nm, 1 nm bandwidth and a scan rate of 1 nm/min. A signal-averaged over three scans were collected. The recorded spectrum was analyzed *in silico* using K2D3[40] online software, and the secondary structure of refolded GSAP_I4 was determined.

Dot-Blot Far-Western. The dot-blot far-Western experiment was performed as reported by Angira et al. in 2019[13] for the canonical GSAP with few modifications. Two microliters of each of the four peptides ^{712}IQ^{727}, ^{719}TT^{743}, ^{734}GY^{757}, ^{746}EN^{770} was adsorbed as a dot on a pre-wetted PVDF membrane at a concentration ranging from 500 to 0 μM. The GSAP_I4 (50 μM), MBP-GSAP isoform 1 (10 μM), and BSA (10 μM) were taken as controls in the same experiment. The drop was allowed to adsorb on the membrane for 1.5 h, and then the membrane was blocked with 5% fat-free milk in TBST for 2 h at room temperature. It was then incubated with 5 mL of 10 μM GSAP_I4 protein diluted in TBST, for 2 h at room temperature followed by anti-PION primary antibody

https://doi.org/10.1021/acsomega.3c01117
ACS Omega 2023, 8, 13435−13443

incubation at 4 °C for 10−12 h. The membrane was incubated with HRP-labeled antirabbit secondary antibody for 2 h at room temperature. ECL from Bio-Rad was used to develop the blot and the result was analyzed in-gel documentation (gel doc) system (Bio-Rad). Extensive washing of the membrane with TBST followed each step three to four times, and the membrane was not allowed to dry in any of the steps.

Indirect ELISA. The 96-well microtiter plates from Corning were coated with 100 μL of peptides with a concentration of 100 μM dissolved in sodium phosphate buffer (pH 8.0) at 37 °C for 2 h. The nonspecific binding sites were blocked with 200 μL of 5% fat-free milk in TBST for 2 h, and later, the wells were loaded with GSAP_I4 protein with a concentration of 10 μM with an incubation for 2 h at room temperature. It was followed by an addition of 50 μL of 1 μg/mL anti-PION rabbit polyclonal antibody in each well and was incubated at 4 °C for 12 h. Fifty microliters of HRP-conjugated antirabbit secondary antibody was then added, and the plate was incubated for 2 h at room temperature with gentle shaking. The final step included the addition of 50 μL of ECL solution (Bio-Rad) that would lead to luminescence. As mentioned in dot-blot far-Western, each step was followed by an extensive washing with TBST for three to four times and the wells was not allowed to dry in any of the steps. The readout for the experiment was the luminescence that was measured using a multimode plate reader (Envision, Perkin Elmer). Four types of controls were used in four different wells that included only GSAP_I4, only peptide, and no GSAP_I4 no peptide and BSA.

GSAP Isoform 4 MD Simulation Studies. The workable models of GSAP_I4 and APP-C99 were generated using Alpha Fold server.[41] The predicted structures were subjected for validation to ERRAT and PROCHECK servers. The validations by PROCHECK were done based on the stereo chemical quality, hydrogen bonding energy, and torsion angles. Based on the interaction of atoms with respect to amino acid residues, ERRAT validates the predicted protein structure by separating correct and incorrect determined structures.[42]

Protein-Peptide Docking. The protein-peptide docking of GSAP_I4 and APP-C99 was achieved using the Piper,[43,44] module of the Bioluminate package (Schrodinger Ltd.), using the OPLS4 force field. Prior to the docking, the protein and the peptide were subjected to protein preparation to optimize the models using PrepWizard. A total of 30 poses were generated. Furthermore, the best docked poses were selected based on their RMSD values.

MD Simulations. The protein-peptide docking of the GSAP_I4 and APP-C99 peptide complex was assessed by performing MD simulation at 500 ns obtained from with periodic boundary conditions, using Desmond[45] (Desmond, Schrödinger, LLC, NY, USA). The system builder panel of Desmond was used to prepare an orthorhombic simulation box in such a way that the boundaries of the box were at least 10 Å away from the protein molecule. The simulation box was solvated with TIP3P explicit water model, and counter-ions were added to neutralize the system. The isosmotic salt environment was provided by adding 0.15 M NaCl. Before starting the simulation, the whole system was minimized with convergence criteria of 1 kcal/mol/Å using an OPLS4 force field. The 500 ns MD simulation using NPT ensemble, at a temperature of 300 K and atmospheric pressure (1.013 bars), with the default setting of relaxation before simulation. Temperature and pressure were maintained constant during simulation using a Nose-Hoover Chain thermostat and a Martyna-Tobias-Klein barostat, respectively. A time step of 0.002 fs was considered during the simulation process. Energies and structures were recorded every 1.2 ps and saved in the trajectory. Lastly, simulation interaction diagrams were generated from the generated trajectory to analyze the results.

■ ASSOCIATED CONTENT

Supporting Information

The Supporting Information is available free of charge at https://pubs.acs.org/doi/10.1021/acsomega.3c01117.

Figure S1 shows pairwise alignment between GSAP isoform 1 and GSAP isoform 4 sequence generated by the T-coffee method; Figure S2 contains the pET32a-(+)-*GSAP_I4* expression construct describing the position of gene fragment in the expression vector and other useful information like antibiotic resistant marker, restriction enzyme sites and tags; western blot and dot-blot images (Figures S7 and S8); Figures S4 and S5 displaying the SDS-PAGE gels for the initial expression of GSAP_I4 at different IPTG concentrations; the secondary structure prediction of GSAP_I4 protein using Psipred (Figure S6); molecular docking, MD simulation and in silico results. the sequencing data for both the GSAP_I4 clones provided as Supporting Data 1; and the mass sequencing data for the GSAP_I4 protein given as Supporting Data 2 (PDF)

■ AUTHOR INFORMATION

Corresponding Author

Vijay Thiruvenkatam − *Discipline of Biological Engineering, Indian Institute of Technology Gandhinagar, Gandhinagar, Gujarat 382355, India;* orcid.org/0000-0003-1044-7626; Email: vijay@iitgn.ac.in

Authors

Deekshi Angira − *Discipline of Chemistry, Indian Institute of Technology Gandhinagar, Gandhinagar, Gujarat 382355, India*

Sonali Chaudhary − *Discipline of Chemistry, Indian Institute of Technology Gandhinagar, Gandhinagar, Gujarat 382355, India*

Arumugam Abiramasundari − *Discipline of Biological Engineering, Indian Institute of Technology Gandhinagar, Gandhinagar, Gujarat 382355, India*

Complete contact information is available at: https://pubs.acs.org/10.1021/acsomega.3c01117

Author Contributions

V.T. conceptualized the idea and designed the project. V.T. and D.A. designed all the experiments and protocols. D.A., S.C., and A.A. performed all the experiments. V.T. and D.A. contributed in writing this manuscript.

Funding

The authors thank Indian Institute of Technology Gandhinagar, India, for lab infrastructure and facilities.

Notes

The authors declare no competing financial interest.

■ ACKNOWLEDGMENTS

We thank IIT Bombay for MASSFIITB facility supported by Department of Biotechnology (BT/PR13114/INF/22/206/

2015). We also thank Dr. Sivapriya Kirubakaran, Assistant Professor at IIT Gandhinagar, India, for her constant inputs. We thank Rashmi Bhakuni and Althaf Shaik, research scholars at IIT Gandhinagar, for the helpful discussions and proofreading the article.

■ ABBREVIATIONS

APP	amyloid precursor protein
Aβ	amyloid β
CD	circular dichroism
ECL	enhanced chemiluminiscence
ELISA	enzyme-linked immunosorbent assay
GSAP_I4	γ-secretase activating protein isoform 4
GSAP	γ-secretase activating protein
IPTG	isopropyl-β-D-1-thiogalactopyranoside
LB	Luria−Bertani
MBP	maltose binding protein
MD	molecular dynamic
MWCO:	molecular weight cutoff
Ni-NTA	nickel nitrilotriacetic acid
OD_{600}	optical density
PION	protein pigeon homologue
PVDF	polyvinylidene fluoride
rpm	revolutions per minute
SDS-PAGE	sodium dodecyl sulfate poly acrylamide gel electrophoresis
SEC-FPLC	size exclusion chromatography-Fast protein liquid chromatography
TBST	tris buffer saline Triton-X
Trx	thioredoxin

■ REFERENCES

(1) Wang, Y.; Liu, J.; Huang, B. O.; Xu, Y.-M.; Li, J.; Huang, L.-F.; Lin, J.; Zhang, J.; Min, Q.-H.; Yang, W.-M.; Wang, X.-Z. Mechanism of Alternative Splicing and Its Regulation. *Biomed. Rep.* **2015**, *3*, 152−158.

(2) Pan, Q.; Shai, O.; Lee, L. J.; Frey, B. J.; Blencowe, B. J. Deep Surveying of Alternative Splicing Complexity in the Human Transcriptome by High-Throughput Sequencing. *Nat. Genet.* **2008**, *40*, 1413−1415.

(3) Nilsen, T. W.; Graveley, B. R. Expansion of the Eukaryotic Proteome by Alternative Splicing. *Nature* **2010**, *463*, 457.

(4) Xie, J.; Black, D. L. A CaMK IV Responsive RNA Element Mediates Depolarization-Induced Alternative Splicing of Ion Channels. *Nature* **2001**, *410*, 936−939.

(5) Stamm, S.; Ben-Ari, S.; Rafalska, I.; Tang, Y.; Zhang, Z.; Toiber, D.; Thanaraj, T. A.; Soreq, H. Function of Alternative Splicing. *Gene* **2005**, *344*, 1−20.

(6) Kontrogianni-Konstantopoulos, A.; Frye, C. S.; Benz, E. J. J.; Huang, S. C. The Prototypical 4.1R-10-KDa Domain and the 4.1g-10-KDa Paralog Mediate Fodrin-Actin Complex Formation. *J. Biol. Chem.* **2001**, *276*, 20679−20687.

(7) Dodt, G.; Warren, D.; Becker, E.; Rehling, P.; Gould, S. J. Domain Mapping of Human PEX5 Reveals Functional and Structural Similarities to Saccharomyces Cerevisiae Pex18p and Pex21p. *J. Biol. Chem.* **2001**, *276*, 41769−41781.

(8) Cieply, B.; Carstens, R. P. Functional Roles of Alternative Splicing Factors in Human Disease. *Wiley Interdiscip. Rev. RNA* **2015**, *6*, 311−326.

(9) Stastna, M.; Van Eyk, J. E. Analysis of Protein Isoforms: Can We Do It Better? *Proteomics* **2012**, *12*, 2937−2948.

(10) Yang, X.; Coulombe-Huntington, J.; Kang, S.; Sheynkman, G. M.; Hao, T.; Richardson, A.; Sun, S.; Yang, F.; Shen, Y. A.; Murray, R. R.; Spirohn, K.; Begg, B. E.; Duran-Frigola, M.; MacWilliams, A.; Pevzner, S. J.; Zhong, Q.; Trigg, S. A.; Tam, S.; Ghamsari, L.; Sahni, N.; Yi, S.; Rodriguez, M. D.; Balcha, D.; Tan, G.; Costanzo, M.; Andrews, B.; Boone, C.; Zhou, X. J.; Salehi-Ashtiani, K.; Charloteaux, B.; Chen, A. A.; Calderwood, M. A.; Aloy, P.; Roth, F. P.; Hill, D. E.; Iakoucheva, L. M.; Xia, Y.; Vidal, M. Widespread Expansion of Protein Interaction Capabilities by Alternative Splicing. *Cell* **2016**, *164*, 805−817.

(11) Bhuiyan, S. A.; Ly, S.; Phan, M.; Huntington, B.; Hogan, E.; Liu, C. C.; Liu, J.; Pavlidis, P. Systematic Evaluation of Isoform Function in Literature Reports of Alternative Splicing. *BMC Genomics* **2018**, *19*, 637.

(12) Wong, E.; Liao, G. P.; Chang, J. C.; Xu, P.; Li, Y.-M.; Greengard, P. GSAP Modulates γ-Secretase Specificity by Inducing Conformational Change in PS1. *Proc. Natl. Acad. Sci. U. S. A.* **2019**, *116*, 6385−6390.

(13) Angira, D.; Chikhale, R.; Mehta, K.; Bryce, R. A.; Thiruvenkatam, V. Tracing the GSAP-APP C-99 Interaction Site in the β-Amyloid Pathway Leading to Alzheimer's Disease. *ACS Chem. Neurosci.* **2019**, *10*, 3868−3879.

(14) He, G.; Luo, W.; Li, P.; Remmers, C.; Netzer, W.; Hendrick, J.; Bettayeb, K.; Flajolet, M.; Gorelick, F.; Wennogle, L. P.; Greengard, P. Gamma-Secretase Activating Protein, a Therapeutic Target for Alzheimer's Disease. *Nature* **2010**, *467*, 95−98.

(15) Hussain, I.; Fabrègue, J.; Anderes, L.; Ousson, S.; Borlat, F.; Eligert, V.; Berger, S.; Dimitrov, M.; Alattia, J.-R.; Fraering, P. C.; Beher, D. The Role of γ-Secretase Activating Protein (GSAP) and Imatinib in the Regulation of γ-Secretase Activity and Amyloid-β Generation. *J. Biol. Chem.* **2013**, *288*, 2521−2531.

(16) Chu, J.; Li, J.-G.; Hoffman, N. E.; Madesh, M.; Praticò, D. Degradation of Gamma Secretase Activating Protein by the Ubiquitin-Proteasome Pathway. *J. Neurochem.* **2015**, *133*, 432−439.

(17) Chu, J.; Li, J.-G.; Joshi, Y. B.; Giannopoulos, P. F.; Hoffman, N. E.; Madesh, M.; Praticò, D. Gamma Secretase Activating Protein Is a Substrate for Caspase-3: Implications for Alzheimer's Disease. *Biol. Psychiatry* **2015**, *77*, 720−728.

(18) Chu, J. Regulation of Gamma-Secretase Activation Protein by the Slipoxygenase: in Vitro and in Vivo Evidence. *Alzheimer's Dement. J. Alzheimer's Assoc.* **2015**, *11*, P372−P373.

(19) Xu, P.; Chang, J. C.; Zhou, X.; Wang, W.; Bamkole, M.; Wong, E.; Bettayeb, K.; Jiang, L.-L.; Huang, T.; Luo, W.; Xu, H.; Nairn, A. C.; Flajolet, M.; Ip, N. Y.; Li, Y.-M.; Greengard, P. GSAP Regulates Lipid Homeostasis and Mitochondrial Function Associated with Alzheimer's Disease. *J. Exp. Med.* **2021**, *218*, No. e20202446.

(20) Hajjari, S. N.; Sadigh-Eteghad, S.; Shanehbandi, D.; Teimourian, S.; Shahbazi, A.; Mehdizadeh, M. MicroRNA-4422-5p as a Negative Regulator of Amyloidogenic Secretases: A Potential Biomarker for Alzheimer's Disease. *Neuroscience* **2021**, *463*, 108−115.

(21) UniProt Consortium. UniProt: A Worldwide Hub of Protein Knowledge. *Nucleic Acids Res.* **2019**, *47*, D506−D515.

(22) Deatherage, C. L.; Hadziselimovic, A.; Sanders, C. R. Purification and Characterization of the Human Gamma-Secretase Activating Protein. *Biochemistry* **2012**, *51*, 5153−5159.

(23) Jones, D. T. Protein Secondary Structure Prediction Based on Position-Specific Scoring Matrices11Edited by G. Von Heijne. *J. Mol. Biol.* **1999**, *292*, 195−202.

(24) Birzele, F.; Csaba, G.; Zimmer, R. Alternative Splicing and Protein Structure Evolution. *Nucleic Acids Res.* **2008**, *36*, 550−558.

(25) Garcia, J.; Gerber, S. H.; Sugita, S.; Sudhof, T. C.; Rizo, J. A Conformational Switch in the Piccolo C2A Domain Regulated by Alternative Splicing. *Nat. Struct. Mol. Biol.* **2004**, *11*, 45−53.

(26) Romero, P. R.; Zaidi, S.; Fang, Y. Y.; Uversky, V. N.; Radivojac, P.; Oldfield, C. J.; Cortese, M. S.; Sickmeier, M.; LeGall, T.; Obradovic, Z.; Dunker, A. K. Alternative Splicing in Concert with Protein Intrinsic Disorder Enables Increased Functional Diversity in Multicellular Organisms. *Proc. Natl. Acad. Sci. U. S. A.* **2006**, *103*, 8390−8395.

(27) Jin, C.; Wang, J.; Wang, Y.; Jia, B.; Guo, X.; Yang, G.; Xu, P.; Greengard, P.; Zhou, R.; Shi, Y. Modulation of Amyloid Precursor Protein Cleavage by \&\#x3b3;-Secretase Activating Protein through Phase Separation. *Proc. Natl. Acad. Sci. U. S. A.* **2022**, *119*, No. e2122292119.

https://doi.org/10.1021/acsomega.3c01117
ACS Omega 2023, 8, 13435−13443

(28) Dehury, B.; Tang, N.; Kepp, K. P. Molecular Dynamics of C99-Bound γ-Secretase Reveal Two Binding Modes with Distinct Compactness, Stability, and Active-Site Retention: Implications for Aβ Production. *Biochem. J.* **2019**, *476*, 1173−1189.
(29) Tang, N.; Somavarapu, A. K.; Kepp, K. P. Molecular Recipe for γ-Secretase Modulation from Computational Analysis of 60 Active Compounds. *ACS Omega* **2018**, *3*, 18078−18088.
(30) Mehra, R.; Kepp, K. P. Understanding Familial Alzheimer's Disease: The Fit-Stay-Trim Mechanism of γ-Secretase. *WIREs Comput. Mol. Sci.* **2022**, *12*, No. e1556.
(31) Shumilin, I. A.; Cymborowski, M.; Chertihin, O.; Jha, K. N.; Herr, J. C.; Lesley, S. A.; Joachimiak, A.; Minor, W. Identification of Unknown Protein Function Using Metabolite Cocktail Screening. *Structure* **2012**, *20*, 1715−1725.
(32) Zhu, H.; Bilgin, M.; Bangham, R.; Hall, D.; Casamayor, A.; Bertone, P.; Lan, N.; Jansen, R.; Bidlingmaier, S.; Houfek, T.; Mitchell, T.; Miller, P.; Dean, R. A.; Gerstein, M.; Snyder, M. Global Analysis of Protein Activities Using Proteome Chips. *Science* **2001**, *293*, 2101−2105.
(33) Pandey, A.; Mann, M. Proteomics to Study Genes and Genomes. *Nature* **2000**, *405*, 837−846.
(34) Notredame, C.; Higgins, D. G.; Heringa, J. T-Coffee: A Novel Method for Fast and Accurate Multiple Sequence Alignment. *J. Mol. Biol.* **2000**, *302*, 205−217.
(35) Tabor, S. Expression Using the T7 RNA Polymerase/Promoter System. *Curr. Protoc. Mol. Biol.* **2001**, *Chapter 16*, Unit16.2.
(36) McCoy, J.; LaVallie, E. Expression and Purification of Thioredoxin Fusion Proteins. *Curr. Protoc. Mol. Biol.* **1994**, *28*, 16.8.
(37) LaVallie, E. R.; McCoy, J. M. Gene Fusion Expression Systems in Escherichia Coli. *Curr. Opin. Biotechnol.* **1995**, *6*, 501−506.
(38) Froger, A.; Hall, J. E. Transformation of Plasmid DNA into E. Coli Using the Heat Shock Method. *J. Vis. Exp.* **2007**, *6*, 253.
(39) Seidman, C. E.; Struhl, K.; Sheen, J.; Jessen, T. Introduction of Plasmid DNA into Cells. *Curr. Protoc. Mol. Biol.* **1997**, *37*, 1.8.
(40) Louis-Jeune, C.; Andrade-Navarro, M. A.; Perez-Iratxeta, C. Prediction of Protein Secondary Structure from Circular Dichroism Using Theoretically Derived Spectra. *Proteins* **2012**, *80*, 374−381.
(41) Jumper, J.; Evans, R.; Pritzel, A.; Green, T.; Figurnov, M.; Ronneberger, O.; Tunyasuvunakool, K.; Bates, R.; Žídek, A.; Potapenko, A.; Bridgland, A.; Meyer, C.; Kohl, S. A. A.; Ballard, A. J.; Cowie, A.; Romera-Paredes, B.; Nikolov, S.; Jain, R.; Adler, J.; Back, T.; Petersen, S.; Reiman, D.; Clancy, E.; Zielinski, M.; Steinegger, M.; Pacholska, M.; Berghammer, T.; Bodenstein, S.; Silver, D.; Vinyals, O.; Senior, A. W.; Kavukcuoglu, K.; Kohli, P.; Hassabis, D. Highly Accurate Protein Structure Prediction with AlphaFold. *Nature* **2021**, *596*, 583−589.
(42) Laskowski, R. A.; MacArthur, M. W.; Thornton, J. M. PROCHECK: Validation of Protein-Structure Coordinates. In *International Tables for Crystallography*; John Wiley & Sons, Ltd, 2012; 684−687.
(43) Chuang, G.-Y.; Kozakov, D.; Brenke, R.; Comeau, S. R.; Vajda, S. DARS (Decoys As the Reference State) Potentials for Protein-Protein Docking. *Biophys. J.* **2008**, *95*, 4217−4227.
(44) Desta, I. T.; Porter, K. A.; Xia, B.; Kozakov, D.; Vajda, S. Performance and Its Limits in Rigid Body Protein-Protein Docking. *Structure* **2020**, *28*, 1071−1081.e3.
(45) Bowers, K. J.; Chow, D. E.; Xu, H.; Dror, R. O.; Eastwood, M. P.; Gregersen, B. A.; Klepeis, J. L.; Kolossvary, I.; Moraes, M. A.; Sacerdoti, F. D.; Salmon, J. K.; Shan, Y.; Shaw, D. E. Scalable Algorithms for Molecular Dynamics Simulations on Commodity Clusters. In *SC 2006 Conference, Proceedings of the ACM/IEEE*; Association for Computing Machinery: New York, NY, United States, 2006; 43.

https://doi.org/10.1021/acsomega.3c01117
ACS Omega 2023, 8, 13435−13443